Evaluation of existing supercritical heat transfer correlations for designing the vapor generator in low-temperature transcritical organic Rankine cycle systems

Jera Van Nieuwenhuyse[1,*], Anastasios Skiadopoulos[2], Dimitris Manolakos[2], Steven Lecompte[1], Michel De Paepe[1]

[1] *Ghent University, Sint-Pietersnieuwstraat 41, 9000 Ghent, Belgium*
[2] *Agricultural University of Athens, Iera Odos 75, 11855 Athens, Greece*

*Corresponding Author: jera.vannieuwenhuyse@ugent.be

ABSTRACT

Transcritical operation of organic Rankine cycle systems for low-temperature heat conversion has gained interest over the last decades due to its performance. Compared to subcritical operation increased, thermal efficiency and higher power output is expected. The design of the supercritical vapor generator in these systems is key to the overall design and operation of the system. Over the years, several supercritical heat transfer correlations have been developed. However, the practical applicability of these correlations has rarely been evaluated. In this work, the performance of several supercritical heat transfer correlations is evaluated based on measurements on a helical coil heat exchanger. This heat exchanger was previously designed and custom-built to work under supercritical conditions and is installed in a small-scale transcritical ORC engine coupled with concentrating photovoltaic thermal collectors. The ORC has a nominal capacity of 3 kWel and the maximum temperature of the heat source (water) is 90°C. R404A was selected as the working fluid, which has a critical temperature and pressure of 72°C and 37.3 bar, respectively. The helical coil heat exchanger is made out of a 66 m long coiled tube with an inner diameter of 0.0257 m. The coil diameter is equal to 0.6 m and the heat exchanger has a nominal capacity of 41 kWth. The prediction capability of several supercritical heat transfer correlations is examined by comparing the measured performance of the helical coil heat exchanger from field tests to the results of simulations based on the (piece-wise) ε-NTU method. Based on this comparison, a best performing correlation is put forward.

1 INTRODUCTION

The performance and efficiency of an organic Rankine cycle (ORC) system can be improved by operating under transcritical conditions. That is why transcritical ORCs, where heat transfer to the high pressure working fluid takes place under supercritical conditions, have gained interest over the last decades. By operating under supercritical conditions, heat transfer losses can be reduced and cooling of the heat source can be increased in the high pressure side heat exchanger (Schuster *et al.*, 2010). The design of this supercritical heat exchanger, called the vapor generator, is key in the overall design and operation of the system. Heat exchangers in general make up a large part of the total exergy loss of a system (Liang *et al*., 2019), so designing it well is important. As the vapor generator also accounts for the largest cost of a transcritical ORC, which can be up to 43% (Lecompte *et al.*, 2015), it is beneficial to limit the oversizing of this component to avoid unnecessary costs. Therefore, the supercritical heat transfer correlations, which are used in the design, should be reliable. Over the years, several supercritical heat transfer correlations have been developed for refrigerants (Van Nieuwenhuyse *et al.*, 2022). However, the practical applicability of these correlations has rarely been evaluated based on the performance of an actual supercritical heat exchanger. Therefore, this work will look into this performance by comparing results from a modeled heat exchanger to experimental results from a heat exchanger incorporated in an experimental test rig. The method used is based on the method of Kaya *et al.* (2018) who did a similar investigation for several two-phase heat transfer correlations.

2 DESCRIPTION OF TEST RIG AND EXPERIMENTAL CAMPAIGN

2.1 Transcritical ORC test rig

The heat exchanger under investigation is part of a small-scale transcritical ORC test rig, with a nominal capacity of 3 kWel and is located in Athens, Greece (37°59'09"N, 23°42'21"E). A schematic diagram of the test rig is given in Figure 1. The ORC is connected to a solar field, consisting of 10 concentrating photovoltaic thermal collectors, with a total nominal heat capacity of 41 kWth. The collectors are equipped with a single-axis solar tracking system and rotate horizontally about an East-West tracking axis. An electric heater (total capacity of 48 kWel) is installed in the circuit to serve as a backup for when the solar irradiation is insufficient to reach test conditions. Water, with a maximum temperature of 90°C, is used as the heat transfer fluid in the circuit connected to the solar connectors. The helical coil heat exchanger is installed in between the water circuit and the ORC circuit and uses R404A as the working fluid. The critical temperature and critical pressure of this fluid are 72°C and 37.3 bar, respectively. A scroll type expander is used, which was modified from a commercial scroll compressor with a volume ratio of 2.8 and a swept volume of 127.1 cm^3, and the refrigerant pump is a triplex diaphragm pump. The rotational speed of the expander and pump is regulated by frequency inverters. The condenser is an evaporative condenser, but when the ORC is not operating, an air chiller is used to dissipate the heat coming from the collectors. The vapor generator is explained in more detail in the next section.

Measurement equipment is installed at different locations in the setup. The most important measurements for the current investigation are pressure and temperature measurements at the in- and outlet of the supercritical heat exchanger and volume flow rate measurements, both on refrigerant and water side. Temperatures were measured with an accuracy of 0.1K, pressures with 0.35 bar (low pressure side) or 0.6 bar (high pressure side). The volume flow rate of the water was measured with an ultrasonic flow meter (accuracy of 1%). The volume flow rate of the refrigerant was calculated using the pump's characteristic (linear correlation between volume flow rate and speed) and the accuracy was estimated at 2% (Kosmadakis *et al.*, 2016).

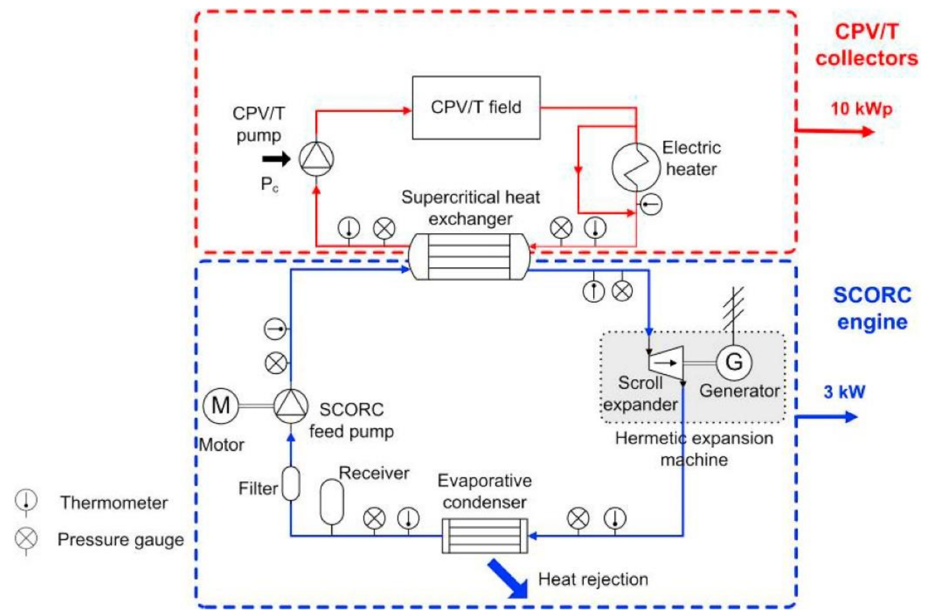

Figure 1: Schematic diagram of the transcritical ORC test rig (Kosmadakis *et al.*, 2016).

2.2 Helical coil heat exchanger layout

The vapor generator of this transcritical ORC was developed for this test rig and supercritical operation specifically (Lazova *et al.*, 2016), and is of the helical coil type with a capacity of 41 kWth. The refrigerant flows upwards in the coil which is placed in an annulus, while the heat transfer fluid (i.e. water) flows downwards in the annulus. Figure 2 shows an illustration of the cross-section of the heat exchanger design. Table 1 gives an overview of the corresponding dimensions.

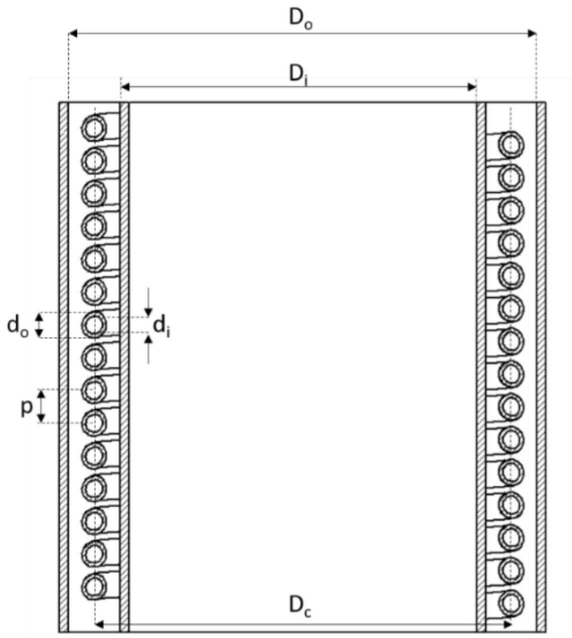

Figure 2: Cross-section of helical coil heat exchanger design.

Table 1: Dimensions of helical coil heat exchanger.

Dimension	Value [m]
Tube inner diameter d_i	0.0257
Tube outer diameter d_o	0.0377
Inner shell diameter D_i	0.526
Outer shell diameter D_o	0.674
Coil diameter D_c	0.6
Pitch p	1.25 d_o
Helical coil tube length L_t	66

2.3 Experimental campaign

In order to reach transcritical conditions (i.e. both temperature and pressure at the outlet of the supercritical heat exchanger on the refrigerant side are above its critical values), measurements were performed on clear and sunny days spread over July, August and September 2021. Solar irradiation under these conditions was maximum at around 1,000 W/m^2. Under these conditions, supercritical pressures could be obtained (for high ORC pump speed and low expander speed), but the temperature at the outlet of the supercritical heat exchanger remained below the critical value. Therefore, the back-up electrical heater was employed almost constantly during the measurements. When starting up, the pressure of the water in the solar collector's circuit was checked and increased if necessary (to reach a pressure of around 3 bar). Next, the evaporative cooler was turned on (and the air-chiller was disabled). The frequency of the water pump was set to 50 Hz. Then, the solar collectors were powered by activating the solar tracking system. When the water cooling down the collectors reached a temperature between 60 to 65°C, the ORC was started. The ORC pump first ran at a low frequency of 10 Hz. Gradually, pressure and temperature in the system increased and pump frequency was increased in a stepwise manner. When the pump frequency was at 20 Hz, the expander was put into operation as well, with a start-up frequency of 10 Hz.

A total of 43 (quasi) steady-state operating points were measured during the experimental campaign, of which 39 were performed under transcritical operating conditions. The refrigerant heat exchanger inlet temperatures ranged from 30.3 to 45.4°C, outlet temperatures from 76.1 to 91.8°C, average pressures from 37.5 to 42.8 bar and mass flow rates from 0.27 to 0.4 kg/s. For the water, inlet temperatures ranged from 81.7 to 94.2°C, outlet temperatures from 76.4 to 88.0°C, average pressures from 3.4 to 4.7 bar and mass flow rates from 2.5 to 2.9 kg/s. Post-processing of the measurements was done with the EES software and Python (version 3.6). A heat balance of the supercritical heat exchanger was calculated in order to estimate the heat losses of the heat exchanger (see Equation (1)). In this equation, $\dot{Q}_{hx,hf}$ is the heat transferred to the ORC in the supercritical heat exchanger on the heating fluid's side. $\dot{Q}_{hx,r}$ is the heat transferred to the ORC in the supercritical heat exchanger calculated on the refrigerant side.

$$dE_{hx,rel} = \frac{\dot{Q}_{hx,hf} - \dot{Q}_{hx,r}}{\frac{\dot{Q}_{hx,hf} + \dot{Q}_{hx,r}}{2}} \tag{1}$$

On average, the heat balance closed within 23.2%. These large deviations in heat balance can be explained by the high heat losses that occur in the heat exchanger. The maximum heat losses that occurred were in the range of 22 kWth. This issue was already highlighted in the work of Golonis *et al.* (2021) and is due to the large uninsulated surface of the supercritical heat exchanger.

3 SIMULATIONS BASED ON ε-NTU METHOD

3.1 Modeling of helical coil heat exchanger

The performance of the heat exchanger was modeled by applying a piece-wise ε-NTU method. Even though, on the global heat exchanger scale, the orientation of the water and refrigerant flow is counterflow (water flows down, refrigerant up), the flow is better approximated by cross-flow on a small-scale level (Kaya *et al.*, 2018). The parameters displayed in Table 1 are used as input to the model. This is complimented with information on the mass flow rates, pressures and inlet temperatures of R404A and water. As the focus of the current work is on the heat transfer, the pressure drop over the heat exchanger is not taken into account into the simulations, and the average pressure is taken as input. For each of the performed simulations, the outlet temperatures of R404A and water are calculated, based on the aforementioned inputs. The total helical coil tube length is divided into parts of equal lengths (L_j) and for every simulation element j, the amount of heat exchanged is calculated with the ε-NTU method based on the overall heat transfer coefficient (U_j, see Equation (2)) between water and R404A for that simulation element. Based on this calculated heat exchange, input temperatures for the next simulation element are calculated. In total, 100 simulation elements were selected as increasing this number from 50 to 100 only resulted in a maximum relative deviation in simulated refrigerant outlet temperature of 0.4%. Therefore, increasing the number of elements even more would not result in more accurate simulations but would increase runtime of the simulations significantly.

$$U_j A_j = \left[\frac{1}{h_{r,j}}\frac{d_o}{d_i} + R_f\frac{d_o}{d_i} + \frac{d_o \ln\left(\frac{d_o}{d_i}\right)}{2\lambda_s} + R_f + \frac{1}{h_{hf,j}}\right]^{-1} * A_j \; with \; A_j = \pi d_o L_j \tag{2}$$

In the Equation 2, R_f represents the fouling resistance (0.176*10^{-6} m^{2}K/W (Kakaç *et al.*, 2012)), λ_s the thermal conductivity of the steel tube (45 W/mK) and h_r and h_{hf} the convection coefficient of the refrigerant and heating fluid (i.e. water), respectively. The properties of R404A and water are calculated with CoolProp v6.3. The shell side convection coefficient h_{hf} is calculated using the calculation method of Patil *et al.* (1982). For the refrigerant side convection coefficient h_r, different correlations are applied in order to find the best suited one for the current conditions. More information on the selected correlations is provided in the next section. In order to compensate for the fact that the refrigerant flow is helical, the following correction factor (developed by Schmidt (1967)) is applied to the refrigerant side heat transfer coefficient:

$$F_{helical} = 1 + 3.6\left(1 - \frac{d_i}{D_c}\right)\left(\frac{d_i}{D_c}\right)^{0.8} \tag{3}$$

This correction factor was also applied by Lazova *et al.* (2016) in the design of the helical coil heat exchanger under consideration in the current work. As the geometry of the heat exchanger falls within the application range of the correlation, it was deemed suited for the current investigation.

The convection coefficients are dependent on the inlet and outlet temperatures of the two fluids of that simulation element. The inlet refrigerant temperature and outlet heating fluid temperature for the j-th simulation element are equal to the outlet refrigerant temperature and inlet heating fluid temperature from the (j-1)-th simulation. The outlet refrigerant temperature and inlet heating fluid temperature of the j-th element need to be determined iteratively. The simulation is started at the bottom of the heat exchanger, so at the refrigerant inlet and heating fluid outlet. The inlet refrigerant temperature is known, and an initial guess has to be made for the heating fluid outlet temperature. After simulating the 100 elements, the actual heating fluid inlet temperature (at the top of the heat exchanger) is compared to the simulated one. If the difference is too big, the initial guess of the heating fluid outlet temperature at the bottom of the heat exchanger is updated and the simulation is run again. The simulation is stopped when the relative difference between the actual heating fluid inlet temperature at the top of the heat exchanger and the simulated temperature is smaller than 0.1%.

The heat losses were not directly modeled, but are taken into account by comparing the measurements to the simulations for the refrigerant side. Comparison based on the heating fluid side would not make sense as in reality the heating fluid side temperatures will always be lower than the simulated ones due to the heat losses. Normally, the actual temperatures of the heating fluid side will thus be different from the simulated ones throughout the heat exchanger. However, this does not have a significant influence on the results of the simulations as the temperature change on the heating fluid side is small (maximum of 6.8°C over the entire heat exchanger), and the properties and thus convection coefficient on the heating fluid side (i.e. water) do not really change for a small change in temperature.

The same type of model has been applied and validated in the work of Kaya *et al.* (2018) for comparing measurements to simulations under subcritical conditions.

3.2 Applied supercritical heat transfer correlations

As mentioned before, the goal of the current work is to evaluate the performance of several supercritical heat transfer correlations. An overview of the selected correlations, together with the intended application range and fluid is given in Table 2. p_{rel} represents the tested pressures relative to the critical pressure of the corresponding fluid, G is the mass flux under consideration expressed in kg/m^{2}s, q the heat flux in kW/m^2 and d_i the inner diameter expressed in mm. The first correlation is the well-known Dittus-Boelter correlation. This correlation is the only one from the selected correlations that is not specifically developed for supercritical flows. It is included in the current study to serve as a reference for subcritical conditions and see if there is a significant improvement in prediction when correlations developed for supercritical flow are applied. The Dittus-Boelter correlation is valid for $0.6 \leq Pr_b \leq 160$, $Re_b \geq 10^4$ and $L/d_i \geq 10$. The correlations of Petukhov *et al*. (1963), Mokry *et al*. (2011) and Garimella (2006) are selected as these correlations were used in the design stage of the current helical coil heat exchanger (Lazova *et al.*, 2016). The correlation of Garimella (2006) and Garimella *et al.* (2015) were developed for cooling heat transfer. However, as they are based on data of the same refrigerant as the current study, they are still interesting to compare to the other correlations. Yu *et al*. (2013) developed a correlation based on data of a large diameter tube of 26 mm, which is very close to the tube in the current investigation (i.e. 25.7 mm). In the work of Yu *et al*. (2013), two correlations were developed for horizontal flow, one for the top of the tube and one for the bottom. These will be depicted as Yt and Yb, respectively.

Based on the simulations explained in Section 3.1, a refrigerant outlet temperature is calculated for each of the tabulated correlations (used to determine the heat transfer coefficient on the refrigerant side). When this outlet temperature is closest to the actual outlet temperature of the corresponding measurement, the correlation is considered as best fitting.

Table 2: Heat transfer correlations for supercritical flow.

Correlation	Symbol	Fluid	p_{rel}	G	q	d_i
Dittus and Boelter (1985)	DB	Water	subcritical	n/a	n/a	n/a
Petukhov *et al.* (1963)	P	CO_2	n/a	n/a	n/a	n/a
Garimella (2006)	Ga	R404A/R410A	1-1.2	200-800	n/a	6.2-9.4
Garimella *et al.* (2015)	Gb	R404A/R410A	1-1.2	200-800	n/a	0.76-9.4
Mokry *et al.* (2011)	M	Water	1.09	200-1500	≤1250	10
Yu *et al.* (2013)	Yt & Yb	Water	1.04-1.13	300-700	200-400	26

4 RESULTS AND DISCUSSION

In total, 39 measurements were performed under supercritical conditions. In Figure 3, the results for the 3rd measurement are displayed, where the correlations' average deviation between simulated refrigerant outlet temperature and the actual outlet temperature is minimal (i.e. 0.6°C). For this measurement, the prediction based on all the correlations is good, and the maximum deviation between simulations and measurements, which is for the Dittus and Boelter (1985) correlation, is only 0.8°C. The best prediction is made by Yu *et al.* (2013) for the bottom of the tube with a difference of only 0.3°C. Very different results are observed for the 13th measurement (see Figure 4). The difference in experimental conditions between the 3rd and 13th measurement are the set frequencies of the pump and expander. For the 3rd measurement, these are 50 Hz and 5 Hz, respectively. For the 13th measurement, these are 60 Hz and 17.5 Hz. This results in a higher mass flow rate for the latter (from 0.33 kg/s to 0.38 kg/s) and a decrease in average refrigerant pressure (from 40.9 to 38.2 bar, which is a lot closer to the critical pressure of 37.3 bar). For the 13th measurement, none of the correlations can predict the outlet temperature very accurately, and the average deviation amounts to 5.4°C. The Petukhov *et al.* (2015) correlation performs the worst, with an underprediction of the outlet temperature with 6.2°C. Again, the prediction of Yu *et al.* (2013) is best, but still underestimates the actual temperature with 4.4°C. In general, over all the measurements, the Yu *et al.* (2013) correlation for the bottom of the tube is best, with an average deviation of 2.6°C, followed by the one from Garimella (2006) with an average deviation of 3°C. The one from Petukhov *et al.* (2015) is worst, with an average deviation of 3.8°C.

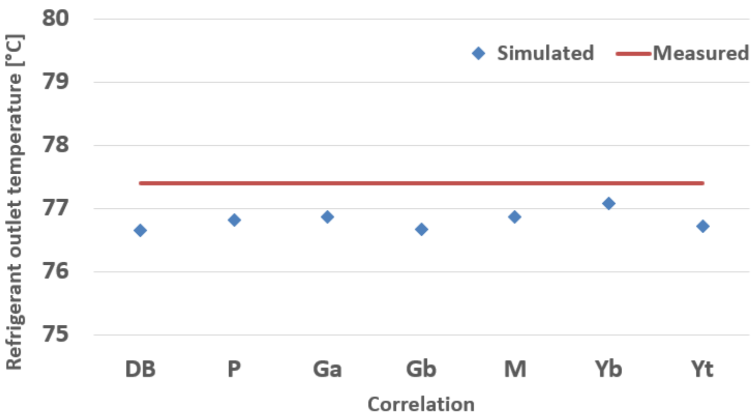

Figure 3: Simulated refrigerant outlet temperatures for 3rd measurement.

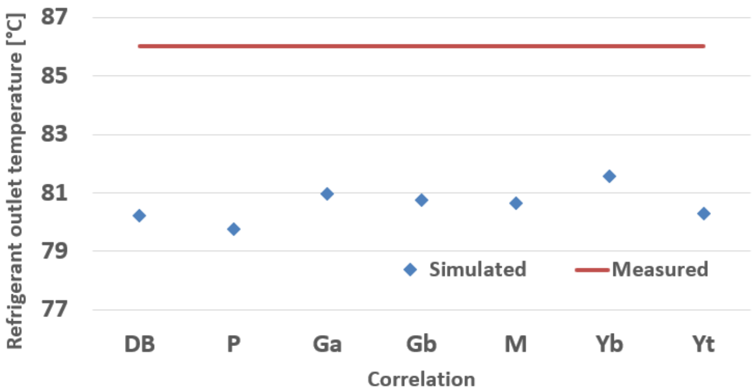

Figure 4: Simulated refrigerant outlet temperatures for 13th measurement.

Similarly, comparison can also be done based on the heat transfer rate. Overall, all the correlations underestimate the actual heat transfer in the heat exchanger. On average, over all the measurements and correlations, the heat transfer rate is underpredicted by 9.5%. The Yu *et al.* (2013) correlation for the bottom of the tube performs best with an average deviation of 7.5%, followed by the one from Garimella (2006) with 8.8%. The Dittus and Boelter (1985) correlation performs worst with an average deviation of 10.6%.

The results shown above indicate that the heat exchanger would be oversized when using the correlations from Table 2 in the sizing. This is illustrated in the following. In Figure 5, the average predicted length of the helical coil tube, based on all the measurements, for every correlation is displayed, together with the actual length of 66 m. On average, the oversizing is equal to 18.9 m. The prediction of Yu *et al.* (2013) for the bottom of the tube is best, but still 14.5 m above the actual tube length of 66 m. Part of the reason for this large oversizing is that in the current results no pinch point temperature difference was defined in the simulations and the actual heat exchanger is also oversized. Therefore, at the outlet of the heat exchanger, the temperature difference between refrigerant and water is very small, both in the simulations and reality. However, in the simulations the heat exchanger is elongated even further in order to realize the total heat transfer rate even though due to the small temperature difference this extra ‘piece’ of heat exchanger does not contribute much. In Figure 6, results are shown when a pinch point temperature difference (dT_{pp}) of 5°C is applied. With incorporating this pinch point temperature, the minimum temperature difference between the refrigerant and heating fluid, which will take place at the outlet of the helical coil tube, is limited to 5°C. In this work, the simulations are performed from the inlet of the tube, and from the moment this threshold is reached, the simulations are stopped. Under these conditions, the average oversizing is 9.1 m and 97% of the actual measured heat transfer rate can be delivered. The prediction by the subcritical correlation of Dittus and Boelter (1985) is worst, however, closely followed by the Petukhov *et al.* (2015) correlation. There is also a visible difference in the prediction of the two correlations from Garimella (Garimella *et al.* (2015) and Garimella (2006)). The best performing correlation of the two (i.e. Garimella (2006)) does not incorporate data on the very small diameter tube of 0.76 mm, which could be an explanation why the prediction is better for the current heat exchanger.

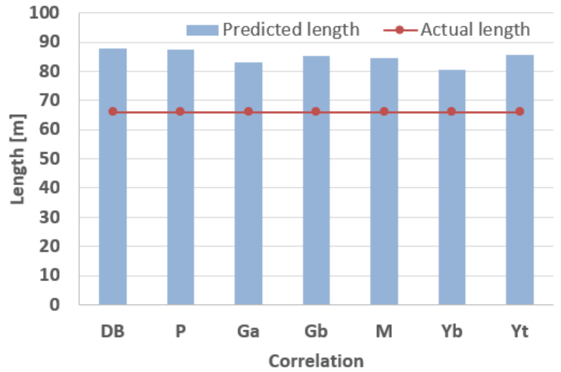

Figure 5: Average predicted length of helical coil tube.

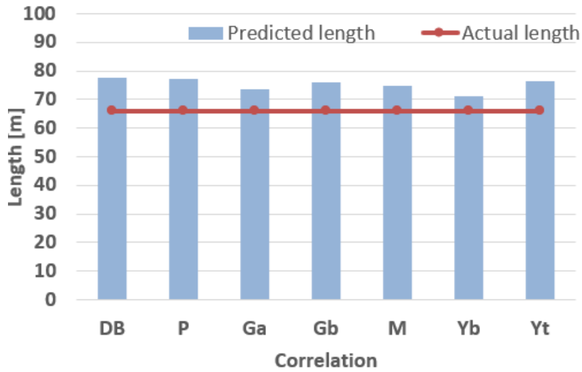

Figure 6: Average predicted length of helical coil tube for a dT_{pp} of 5°C.

In Figure 7, the heat transfer coefficient of refrigerant is illustrated for every correlation (averaged over the 100 simulation elements) and for every measurement. The average prediction of all the correlations together is also displayed. Here, it is clear why the predictions from the Yu *et al.* (2013) correlation (for the bottom), followed by the correlation of Garimella (2006), are best (following from Figure 6). Compared to the predictions of the other correlations and the average prediction of the correlations, the refrigerant side heat transfer coefficient is a lot higher. This results in a higher overall heat transfer coefficient (Equation (2)) between refrigerant and heating fluid, and thus in a smaller required element length L_j, leading to less oversizing of the entire tube length.

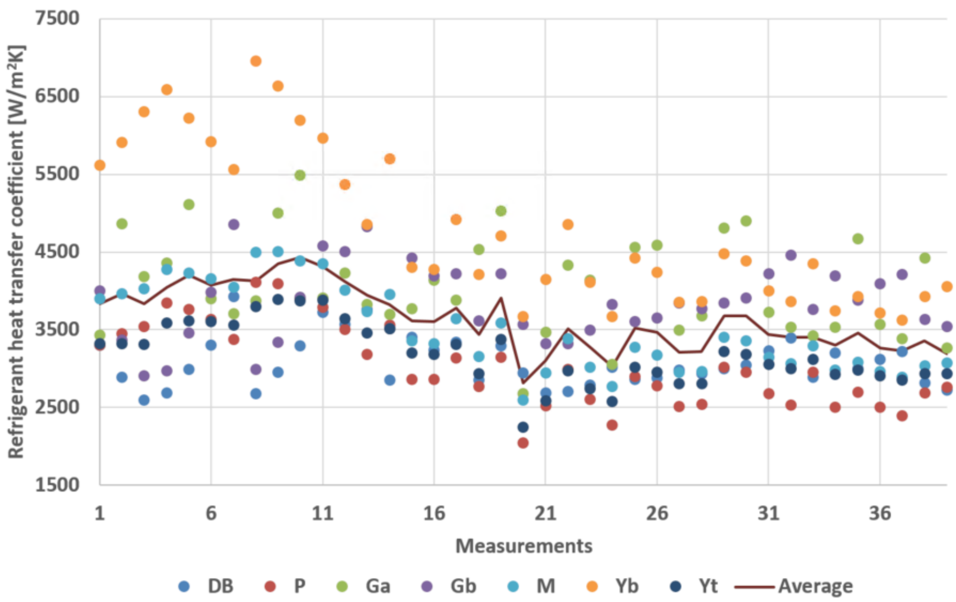

Figure 7: Average refrigerant side heat transfer coefficient for all 39 measurements.

CONCLUSION

In this work, the performance of several supercritical correlations is evaluated by comparing piece-wise simulation results to field tests performed on a helical coil heat exchanger designed to work under supercritical conditions. The measurements are used as input to the model, and based on the correlations, the refrigerant outlet temperature and the total heat transfer rate can be determined. By comparing these results to the actual measurements, a best performing correlation can be put forward.

- All correlations underpredict the refrigerant outlet temperature. The Yu *et al.* (2013) correlation for the bottom of the tube, which is based on large diameter tube data, is best, with an average

deviation of 2.6°C, the one from Petukhov *et al.* (2015) is worst, with an average deviation of 3.8°C.
- For the total heat transfer rate in the heat exchanger, the average underestimation is 9.5%. The correlation of Yu *et al.* (2013) for the bottom has the smallest average deviation of 7.5% and the correlation of Dittus and Boelter (1985) has the largest average deviation of 10.6%.
- In sizing the heat exchanger, the correlation from Yu *et al.* (2013), developed for the bottom of the tube and, performs best. The correlation of Dittus and Boelter (1985) performs the worst, closely followed by the correlation of Petukhov *et al.* (1963).
- For the correlations developed by Garimella (Garimella *et al.* (2015) and Garimella (2006)), Garimella (2006) does not incorporate data on the very small diameter tube of 0.76 mm, and performs best. This indicates that correlations developed for larger diameter tubes are required in order to make a reliable design.

The correlations can perform adequately when predicting refrigerant outlet temperatures. It is however important to simulate different working conditions (varying mass flow rates of refrigerant and heating fluid, varying pressures, varying inlet temperatures, etc.) as the prediction capability can vary for different conditions. However, when using the correlations to size the heat exchanger, all the correlations significantly overpredict the actual required length. The importance of applying a pinch point temperature is illustrated as this already improves the prediction.

NOMENCLATURE

Δ	difference	(/)	U	overall heat transfer coefficient	(W/m^2K)
λ	thermal conductivity	(W/mK)	b	bulk	
A	heat transfer area	(m^2)	c	coil	
d	tube diameter	(m)	el	electrical	
D	shell diameter	(m)	f	fouling	
dE	error on energy balance	(/)	hf	heating fluid	
F	correction factor	(/)	hx	heat exchanger	
G	mass flux	(kg/m^2s)	i	inner	
L	length	(m)	j	number of simulation element	
p	pitch	(m)	o	outer	
Pr	Prandtl number	(/)	pp	pinch point	
q	heat flux	(W/m^2)	r	refrigerant	
$\dot{Q}$	heat transfer rate	(W)	rel	relative	
R	thermal resistance	(m^2K/W)	s	steel	
Re	Reynolds number	(/)	t	total	
T	temperature	(K)	th	thermal	

REFERENCES

Dittus, F., & Boelter, L., 1985, Heat transfer in automobile radiators of the tubular type, *Int. Commun. Heat Mass Transfer*, vol. 12(1), 3-22.

Garimella, S., 2006, High condensing temperature heat transfer performance of low critical temperature refrigerants, *Air-Conditioning and Refrigeration Technology Institute.*

Garimella, S., Mitra, B., Andresen, U.C., Jiang, Y., & Fronk, B.M., 2015, Heat transfer and pressure drop during supercritical cooling of HFC refrigerant blends, *International Journal of Heat and Mass Transfer,* vol. 91, 477-493.

Kakac, S., Liu, H., & Pramuanjaroenkij, A., 2012, *Heat exchangers: selection, rating, and thermal design*, CRC press, third edition.

Kaya, A., Lazova, M., Kosmadakis, G., Lecompte, S., & De Paepe, M., 2018, Evaluation of existing heat transfer correlations in designing helical coil evaporators for low-temperature organic Rankine cycles via inverse design approach, *Heat Transfer Engineering*, vol. 40, 1137-1152.

Kosmadakis, G., Landelle, A., Lazova, M., Manolakos, D., Kaya, A., Huisseune, H., … & Papadakis, G., 2016, Experimental testing of low-temperature organic Rankine cycle (ORC) engine coupled with concentrating PV/thermal collectors: Laboratory and field tests, *Energy*, vol. 117, 222-236.

Lazova, M., Huisseune, H., Kaya, A., Lecompte, S., Kosmadakis, G., & De Paepe, M., 2016, Performance evaluation of a helical coil heat exchanger working under supercritical conditions in a solar organic Rankine cycle installation, *Energies*, vol. 9(6), 432.

Lecompte, S., Lemmens, S., Huisseune, H., Van den Broek, M., & De Paepe, M., 2015, Multi-objective thermo-economic optimization strategy for ORCs applied to subcritical and transcritical cycles for waste heat recovery, *Energies*, vol. 8(4), 2714-2741.

Liang, Y., Bian, X., Qian, W., Pan, M., Ban, Z., & Yu, Z., 2019, Theoretical analysis of a regenerative supercritical carbon dioxide Brayton cycle/organic Rankine cycle dual loop for waste heat recovery of a diesel/natural gas dual-fuel engine, *Energy Conversion and Management*, vol. 197, 111845.

Mokry, S., Pioro, I., Farah, A., King, K., Gupta, S., Peiman, W., & Kirillov, P., 2011, Development of supercritical water heat-transfer correlation for vertical bare tubes, *Nucl. Eng. Des.*, vol. 241, 1126-1136.

Patil, R.K., Shende, B.W., & Ghosh, P.K., 1982, Designing a helical-coil heat exchanger, *Chemical Engineering*, vol. 89(25), 85-88.

Petukhov, B.S., Krasnoshchekov, E.A., Protopopov, V.S., 1961, An investigation of heat transfer to fluids flowing in pipes under supercritical conditions. *International Developments in Heat Transfer*, 1961 International Heat Transfer Conference, ASME, University of Colorado, Boulder, CO, USA, January 8-12, Part III, Paper 67, 569-578.

Schmidt, E.F., 1967, Wärmeübergang und druckverlust in rohrschlangen, *Chemie Ingenieur Technik*, vol. 39(13), 781-789.

Van Nieuwenhuyse, J., Lecompte, S., & De Paepe, M., 2022, Current status of the thermohydraulic behavior of supercritical refrigerants: a review, *Applied Thermal Engineering*, vol. 218, 119201.

Yu, S., Li, H., Lei, X., Feng, Y., Zhang, Y., He, H., & Wang, T., 2013, Experimental investigation on heat transfer characteristics of supercritical pressure water in a horizontal tube, *Experimental Thermal and Fluid Science*, vol. 50, 213-221.

ACKNOWLEDGEMENT

The work presented in this paper was funded by an FWO – Flanders grant (1SA3720N) for strategic basic research of the Research Foundation Flanders. This financial support is gratefully acknowledged. I would also like to thank Tom Catternan and Marnix Van Belleghem for their work on the design and construction of the helical coil heat exchanger.